FAA-AEE-08-02
Federal Aviation Administration
Office of Environment and Energy
800 Independence Ave., SW
Washington, D.C. 20591

FINAL REPORT

LIDAR MEASUREMENT OF EXHAUST PLUME CHARACTERISTICS FROM COMMERCIAL JET TURBINE AIRCRAFT AT THE DENVER INTERNATIONAL AIRPORT

Roger L. Wayson
Gregg G. Fleming
George Noel
John MacDonald
U.S. Department of Transportation
Research and Special Programs Administration
John A. Volpe National Transportation Systems Center
Environmental Measurement and Modeling Division, DTS-34
Air Quality Facility, Kendall Square
Cambridge, MA 02142-1093

Wynn L. Eberhard
Brandi McCarty *
Richard Marchbanks *
Scott Sandberg
Joanne George *
NOAA Earth System Research Laboratory
Chemical Sciences Division
R/CSD3 – NOAA
325 Broadway
Boulder, Colorado 80305-3337

* Cooperative Institute for Research in Environmental Sciences
University of Colorado

Draft Report

September, 2007
Revised January, 2008
Revised April, 2008

U.S. Department of Transportation
Federal Aviation Administration

ACKNOWLEDGEMENTS

Denver International Airport personnel were invaluable in selecting the right airfield location to take the measurements and providing security escorts for each day of operation. Additionally, they graciously supplied diesel fuel for portable generators that were used to supply power in the field. In sum, they were the perfect hosts that enabled this project to be a success. The Team would like to specifically thank the efforts of:

- DIA Planning – Rick Busch and Jeannette Stoufer
- DIA Environmental Services – Janell Barrilleaux, Aaron Frame, Bob Nixon, Jerry Williams, Debe Loya, John Hambright, Craig Schillinger, Tracy Schilz, Rick Langlois, Mary Lou Lopez, Keith Pass, Tom Somers, Paul Titus, Sue Davidson, Lindsay Bethel, & Aimee Fenlon
- DIA Airside Operations – Steve Lee, Mark Kullas, and staff
- DIA Field Maintenance – Ron Morin, Jeff Bartleson, and staff
- DIA Fleet Maintenance – Chuck Smith and staff
- DIA Contract Maintenance – April Henderson and Charyn Billick
- DIA Deputy Manager of Aviation – Hana Rocek
- DIA Manager of Aviation – Turner West

EXECUTIVE SUMMARY

Working in close coordination with Denver International Airport (DEN) airport staff, three organizations conducted a LIDAR (LIght Detection And Ranging) measurement study from October 10, 2006 until October 13, 2006, at the DEN. The participants, known as the "Team" were:

- The Volpe National Transportation Systems Center (Volpe), Environmental Measurement and Modeling Division
- The National Oceanic and Atmospheric Administration (NOAA) with the University of Colorado's Cooperative Institute for Research in the Environmental Sciences
- The Federal Aviation Administration, Office of Environment and Energy (AEE)

This is the third in a series of measurements on this topic with the first two conducted at Los Angeles International Airport (LAX) and Atlanta's Hartsfield-Jackson International Airport (ATL). A major goal in all three studies has been to measure the initial plume characteristics of jet exhaust in support of obtaining increased accuracy in air dispersion modeling efforts. All three studies have resulted in cross-sections of the plume which can be quantified and visualized giving initial plume characteristics including plume rise, horizontal plume standard deviation, and vertical plume standard deviation.

DEN was chosen for this latest measurements study because it is unique in some ways, and yet similar to other airports where LIDAR data have been collected. DEN is a unique U.S. airport due to the high altitude of the airport, ranging around a value of 5,431 feet ASL (1,655 meters). Prior LIDAR measurements at LAX and ATL were closer to sea-level with elevations centered near 126 and 1,026 feet ASL, respectively. Also, DEN usually has a much lower relative humidity in October than other airports where testing has occurred, resulting in improved measurement conditions due to the slightly lower air density (due to higher altitude and lower humidity). This results in improved plume detection against a background of less ambient aerosol loading.

Although each LIDAR study resulted in cross-sections of the aircraft jet turbine exhaust plume during takeoff roll, the DEN study offered additional insights into aircraft plume behavior, and data for more accurate modeling of plume rise and spread primarily due to a better understanding of the phenomenon and measurement needs from previous studies. Added to the LAX and ATL results, DEN provides a more robust data set.

In general, the DEN results tend to validate the previous findings. It is still obvious that substantial plume rise occurs and values for initial plume spread are of the same order of magnitude as previously found. However, the analysis of plume characteristics shows slightly different characteristics, most likely due to local airport influences. To fully quantify and reduce uncertainty for plume rise and plume spread so that it could be used in a generic fashion for use at any airport, additional data from other airports are needed because three average parameter data points from each airport are not enough to statistically prove differences.

Current values in use are only from LAX. It is concluded by the Team that the use of average values from all three airports, including a degree of uncertainty by including one-half of the derived ranges, would lead to more accurate dispersion analysis and a determination of the accuracy of the input

variables and provide the uncertainty that is included in this input variable. The values now is use are:

- Plume Rise: 12.0 meters
- σ_y: 10.5 meters
- σ_z: 4.1 meters

The recommended replacement values are:

- Plume Rise: 10.8 ± 1.9 meters
- σ_y: 12.5 ± 2.7 meters
- σ_z: 4.8 ± 1.0 meters

Note: Plume rise is in relation to the ground plane, not the height of the engine.

The exception to this recommendation are the airports where testing has occurred. It is recommended that these three airports use the actual values derived for their own airports.

The changes in standard deviation would result in over a 39 percent increase in plume area at the initial modeling point. Since plume spread and concentration estimates are inversely proportional in the result from these parameters would be a lower predicted concentration. Of course with distance the difference would become smaller but the new parameters would always result in lower concentrations. However, the smaller plume rise, combined with a greater σ_z would increase ground level concentration (defined as 1.6 meters above the ground) at the initial modeling point. Downwind the differences would be less but concentrations would always be greater in flat terrain. The overall effect, in the near field, would be to increase predicted concentrations but detailed modeling is needed to truly evaluate the effects, especially at greater distances.

The DEN measurements have also advanced the idea of separating aircraft based on airframe and engine mounting differences. If assumed to be independent variables, this could further improve the accuracy of dispersion estimates. In terms of engine mount location and larger aircraft vs. commuters, it was shown that the distributions appear to be separate but overlap. As such, it cannot statistically be proven that these are independent data distributions but it appears likely. While the Team would recommend more data before any final decisions are made, if this were to be implemented the recommended values would be:

Wing Mounted Large Commercial Aircraft

- Plume Rise: 10.4 meters
- σ_y: 13.9 meters
- σ_z: 4.7 meters

Fuselage Mounted Large Commercial Aircraft

- Plume Rise: 12.9 meters
- σ_y: 11.8 meters
- σ_z: 5.5 meters

Commuter Aircraft

- Plume Rise: 7.6 meters
- σ_y: 9.6 meters
- σ_z: 3.1 meters

The analysis for meteorological impacts was advanced in the DEN measurements since more meteorological data were available than in previous measurements. Wind shear within a defined height was shown to be an important parameter for plume rise. There was poor correlation for temperature, wind speed and direction when directly compared to plume rise, but the wind shear analysis suggests that additional data would allow for a more in depth analysis of these parameters, and suggests a need for the measurement of lapse rate in the immediate vicinity of the sampling and at the plume rise height. As with previous airports, the DEN results again indicate that thermal buoyancy is a critical factor in plume rise.

To advance these hypotheses, more testing is needed at other airports and minor changes to the collection methodology have been identified. These include:

- Direct determination of atmospheric stability, either by temperature at two heights with precision, aspirated thermometers along with wind speed, or a ambient vertical heat flux and wind measurement.
- Continue exploring trends of different aircraft engine mount locations and the effects on exhaust plume size and plume rise through additional measurements.
- The data tends to indicate that the dispersion parameters from commuter jet aircraft could be modeled independently because of the difference in spread and plume rise, although it cannot be absolutely proved statistically at this time. Additional testing could provide the information for a decision that could be backed by statistical analysis.
- Division of the commuter class into a large (over a specific number of seats) and small (under the same specific number of seats) for continued analysis of future data and retro analysis of the existing data.
- Separation of the fuselage mounted aircraft into more specific categories based on size such as small commuter, large commuter, and large commercial jetliner.
- Evaluation of the plume rise by aircraft type based on the exhaust heat flux for future measurements and retro analysis of existing data. This would require using existing data in a meaningful way. Initial thoughts include the use of a mixed variable from the thrust and fuel flow parameters found in the ICAO Databank.

In terms of future work, the data from all three airports for the in-situ airfield measurements are being combined into a single database. As the number of airports sampled increases, the results will become more applicable when applied in a generic fashion. This is primarily due to the gradual elimination of site bias due to averaged results over different airports. Sensitivity studies should be performed on EDMS which uses the EPA's AERMOD Gaussian dispersion model, to allow a analysis of the changes that occur from including the LIDAR initial plume parameters. If this is also compared to measured data, improvements in the model accuracy could be documented.

The Team concludes that additional measurements should be carried out to evaluate potential changes in the derived parameters to reduce the error due to site characteristics (site bias). Additional measurements would continue to expand the database and improve the derived parameters for plume characteristics (plume rise and initial plume spread). These follow-on studies will be important to:

- Allow further exploration of plume rise variables, especially in late stages of the plume's evolution, and confirm that the exhaust gas temperature may be directly correlated.
- Provide a more extensive data set to allow the analysis of the effects of aircraft types and atmospheric stability to be more accurately defined.
- Allow the inclusion of more detailed meteorological data such as lapse rate in the immediate vicinity of the testing and at the appropriate height.
- Allow for continued development of remote sensing of mass in future sampling

Each data set has added to the body of knowledge and improved the understanding of the characteristics of plumes emitted by jet turbine aircraft. But variations in the data from each airport are evident, leading to uncertainty unless these can be quantified and tied to local variables. Additional measurements will continue to reduce this uncertainty, and lessons learned from previous measurement campaigns have improved each subsequent measurement. Theory has continued to be employed to quantify differences from each airport. The research from the three airports has dramatically increased our understanding of the correct sampling methods (both LIDAR and local variables) and our understanding of plume behavior. The benefits of remote sampling of jet aircraft emissions have yet to be fully realized but offer a relatively low cost alternative to the measurement of aerosols from aircraft.

TABLE OF CONTENTS

(to be included in final copy due to changes that are certain to occur)

INTRODUCTION

The Federal Aviation Administration's (FAA) Office of Environment and Energy, in conjunction with the U.S. Department of Transportation (DOT) Volpe Center (Environmental Measurement and Modeling Division), and the National Oceanic and Atmospheric Administration (NOAA) Earth System Research Laboratory (partnered with the Cooperative Institute for Research in Environmental Sciences) conducted a LIDAR (LIght Detection And Ranging) measurement study from October 10, 2006 until October 13, 2006, at the Denver International Airport (DEN). This is the third in a series of measurements on this topic[1,2] with the first two conducted at Los Angeles International Airport (LAX) and Atlanta's Hartsfield-Jackson International Airport (ATL). A major goal in all three studies has been to measure the initial plume characteristics of jet exhaust in support of obtaining increased accuracy in air dispersion modeling efforts. All three studies have resulted in cross-sections of the plume, which can be quantified and visualized given initial plume characteristics including plume rise, horizontal plume standard deviation, and vertical plume standard deviation.

DEN was chosen for this measurement study because it is unique in some ways, and yet similar to other airports where LIDAR data have been collected. DEN is a unique U.S. airport due to the high altitude of the airport, ranging around a value of 5,431 feet ASL (1,655 meters). Prior LIDAR measurements at LAX and ATL were closer to sea-level with elevations centered near 126 and 1,026 feet ASL, respectively. Also, DEN has a much lower relative humidity in October than other airports where testing has occurred, as shown in Figure 1.[3] LIDAR measurements at DEN benefitted from the decreased air density due to higher altitude and lower humidity, resulting in lower interference of backscatter for the LIDAR measurements due to "cleaner" air (both from dry aerosol loading and lower hygroscopic growth).

Figure 2 shows DEN has about the same average temperature in October as the two airports being studied using LIDAR in the United Kingdom, but a lower average temperature than other airports where measurements have occurred in the U.S. It was thought that these meteorological factors at DEN would allow a better comparison for coordinating LIDAR conclusions from the U.S. and the U.K. research teams, while also providing an additional U.S. data set with different characteristics than those previously measured.

---

[1] Wayson, R.L., G.G. Fleming, B. Kim, W.L. Eberhard, W. A. Brewer, Final Report, The Use of LIDAR to Characterize Aircraft Initial Plume Parameters, FAA-AEE-04-01, **DTS-34-FA34T-LR3**, **Federal Aviation Administration**, Office of Environment and Energy, Washington, D.C. , February, 2004.

[2] Wayson, R., G.G. Fleming, G. Noel, W.L. Eberhard, W.A. Brewer, Measurement of Exhaust Plume Characteristics and Particulate Matter Mass Emissions from Commercial Jet Turbine Aircraft: The UNA UNA Study, FAA-AEE-06, DTS-34-FA34T-LR2, Federal Aviation Administration, Office of Environment and Energy, Washington, D.C., October, 2006.

[3] AEDT database, Sept., 2007

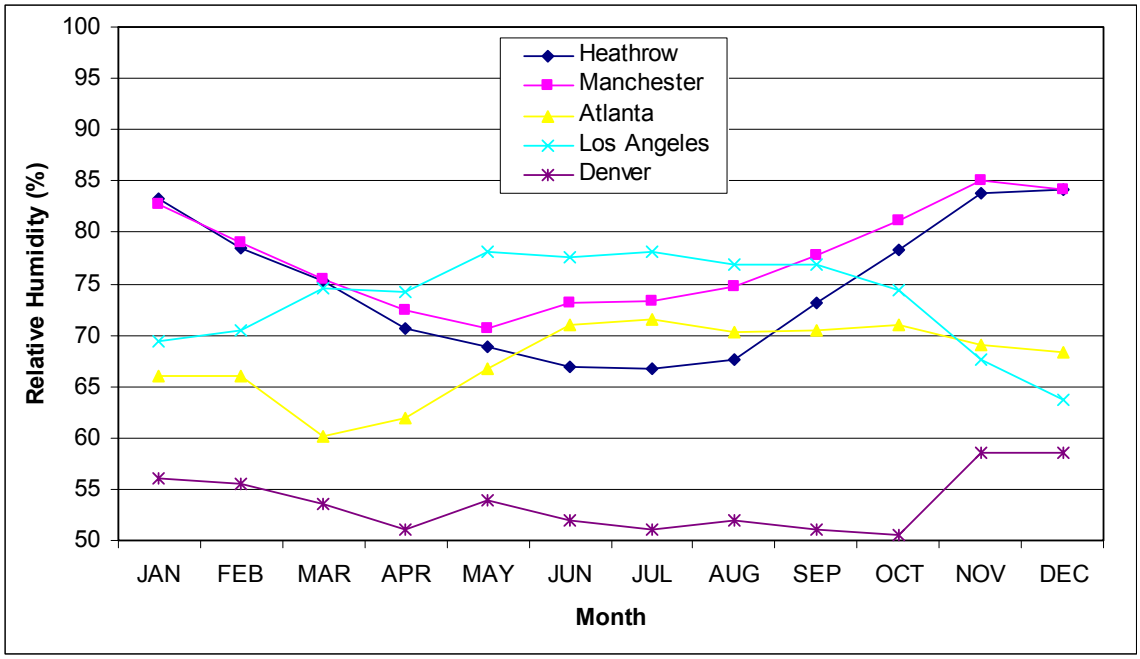

Figure 1. Plot of Relative Humidity for Various Airports[3]

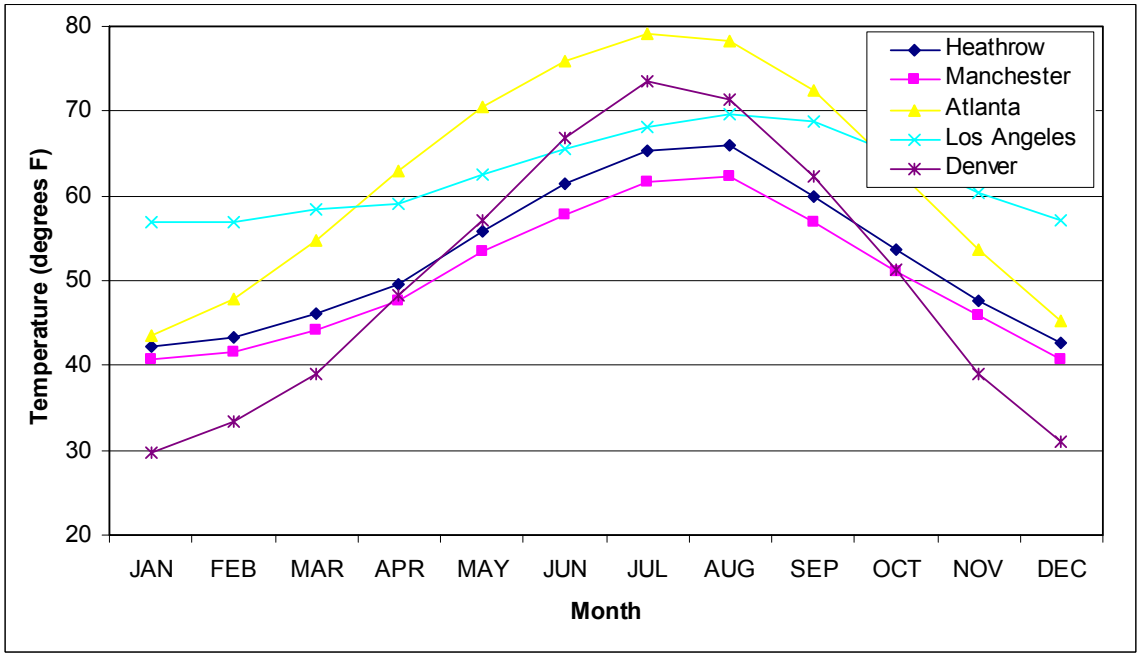

Figure 2. Plot of Temperature for Various Airports[3]

All of these factors made DEN an excellent choice for this LIDAR measurement campaign. Additionally, the measurements and analysis provided on-site data for DEN to consider in future dispersion modeling, which should lead to more accurate results.

This report describes the data collected, analysis and conclusions for the plume parameterization using the LIDAR system for data collection.

PARTICIPANTS

Working in close coordination with DEN airport staff, three organizations conducted the measurements, known as the "Team":

- The Volpe National Transportation Systems Center (Volpe), Environmental Measurement and Modeling Division
- The National Oceanic and Atmospheric Administration (NOAA), including personnel from the Cooperative Institute for Research in Environmental Sciences (CIRES)
- The Federal Aviation Administration Office of Environment and Energy (AEE)

Volpe was responsible for the coordination of the field work, ambient monitoring, final data analysis, and reporting. NOAA was in control of all LIDAR equipment, quality control of data collection, initial analysis and initial data formatting. The sponsor, AEE took an active role in the field work and was critical to the coordination of the Team's needs with the airport staff.

MEASUREMENTS

Before any data were collected, the Team developed a full measurement protocol and considered responses from all participants. Additionally, with the support of DEN staff, the Team conducted a detailed field reconnaissance to assess the various airport locations conducive to the best measurement results. It was decided that the north end of Runway 08/26 (Runway 08) was the best choice because of the local topography, access to the measurement location, non-interference with airport operations, and a measurement location was available at an appropriate distance from the active runway with an unobstructed line of sight.

Three locations were identified at Runway 08/26, shown on Figure 3 as A, B and C. Location A was the primary location and it permitted measurement of a cross-section of the plume at a near 90 degree angle to the path of the aircraft on takeoff. This would allow direct comparison to measurements that had previously been performed at other airports. Location B was selected as a possible place to measure a cross-section of the plume parallel to the runway and aircraft movement. This cross-section, offset to the prevailing downwind side of the runway, was thought to allow better characterization of the plume as a function of aircraft speed during takeoff. This same idea applied to

Figure 3. Denver International Airport Showing Final Measurement Locations

Location C, but Location C was considered more specific for tire/brake particulate matter emissions that are generated during landings. However, the benefits of both locations B and C were secondary to the primary goal of the project, and because of resource limitations and weather complications, were eventually dropped from consideration.

Accordingly, Location A became the base station where the LIDAR system was located. NOAA supplied a diesel generator to supply electrical power, and DEN provided the fuel to supply electrical power. Weather stations were established for microscale measurements and the opportunity to measure $PM_{2.5}$ was taken to measure local concentrations. $PM_{2.5}$ results are reported in a separate document.

Measurements were conducted from October 10, 2006 until October 13, 2006 with setup and takedown occurring before and after these dates. Measurements were made beginning with the first departure bank of the day and often continued well into the evening hours. *No disruption of air traffic was necessary since no special considerations of the operations were needed.*

LIDAR Measurements

Location A provided an almost ideal position for the LIDAR system, called the *Ozone Profiling Atmospheric* LIDAR (OPAL). This was the same system used in the two previous studies[1] with minor modifications made to improve its performance in the jet exhaust measurements. Measurements at this position allowed OPAL to establish a scan plane of takeoffs on the heavily used Runway 08. The scan plane for these measurements was a vertical plane intersecting the aircraft plume at a near perpendicular angle. The use of this scan plane resulted in a measured cross section of the plume perpendicular to the aircraft takeoff roll direction. Continued sweeps[4] of the LIDAR system for this scan plane allowed the plume to be followed as it matured and dissipated behind the aircraft.

The OPAL system location and the associated scan plane are shown in Figure 4. Figure 5 is a picture of the LIDAR system on location and shows the external optical system on the roof along with the meteorological tower employed by NOAA.

LIDAR airfield measurements at DEN were accomplished in a similar manner as for the two previous studies at LAX and ATL. The OPAL LIDAR system operates at an ultraviolet wavelength of 0.355 μm and measures the backscatter from aerosols emitted by the aircraft engines. The measured aerosol components in the jet turbine exhaust plume are very small, with the size distribution peaking typically at 30 and 100 nanometers in diameter. More complete details of the LIDAR system are included in the two previous reports summarizing the measurements.[1,2] NOAA performed all LIDAR

[4] Nomenclature used in this document refers to the vertical plane of LIDAR activity as the scan plane and an entire measurement of an aircraft as a scan. During each scan of an aircraft, multiple sweeps of the scan plane occur as the LIDAR beam traverses up and down in the scan plane. Each sweep results in a measured two-dimensional data array representing the back scatter of a cross section of the aircraft plume providing information on location and dimensions. Accordingly, as defined in this paper, a scan is an entire measurement of an aircraft that includes multiple sweeps while a sweep is a reported data array during one beam traverse of the scan plane.

Figure 4. OPAL Location in Relation to Runway 08 and Scan Plane (Ambient PM2.5 and anemometer general area also shown)

Figure 5. OPAL System Showing Aircraft on Near Taxiway (Runway 08/26 in Far Background)

testing as well as frequent calibrations, initial quality control, and data reduction of the measurements. In-situ aircraft events were measured depending on the time aircraft departed from Runway 08. A LIDAR measurement was begun once a spotter (located nearby but outside of the measurement trailer) and the LIDAR operator (viewing a closed-circuit television monitor) were satisfied that a good event (aircraft takeoff) was about to occur. The spotter, in radio contact with the LIDAR operator, identified the aircraft type approaching and the tail number. This information was both recorded by the spotter and transmitted to the LIDAR operator for a second logging of the event identifiers. Run numbers were also recorded by both and used to help in later identification of the events. After notification by the spotter that an aircraft was beginning its takeoff roll, the LIDAR scan was initiated. A video camera was used to film all takeoff events during measurements and later used during data analysis.

The LIDAR measurement sweeps were continued in the scan of the aircraft plume until the plume dissipated beyond measurement capabilities or another aircraft affected the plume in the scan plane. The measurement data from each sweep were recorded to digital audio tapes (DAT). The data from the tapes were then transferred a desktop personal computer for later processing. After each aircraft scan event, the system was reset and the process repeated.

Since no special movement of aircraft was required in order to perform the measurements, the measured events reflect typical takeoff of many different aircraft airframes and engines. The Team was unable to distinguish between derated versus maximum power takeoffs with the information available and as such, this variable was not considered.

Microscale Meteorological Measurements

At the previous airports, weather data were collected by the airport at a single location and at 10 meters above ground level. This single position was used during analysis at these airports. No correlation of the weather and effect on the plume characteristics was shown during these previous analyses although in theory effects should occur. It was concluded that the weather measurements needed to be more detailed and localized to see any real impact on plume characteristics. To this end, local wind speed and direction were measured at the location by the research team to supplement airport measurements. Additionally, local measurements of the Low Level Windshear Alert System (LLWAS) were also supplied by the airport permitting local wind speed and direction to be measured by several different instruments and at multiple locations.

The Team measured wind parameters at three positions. A cup anemometer to determine wind speed and wind vane for direction determination were mounted at a height of 7.5 meters to a tower mounted on the OPAL trailer (see Figure 5). This information was downloaded directly to computers inside the OPAL trailer.

3-D sonic anemometers, at two heights, were located nearby on independent towers 1.8 and 10 meters above the ground plane (see Figures 6 and 7) to provide both wind speed

Figure 6. Sonic Anemometer at 1.8 Meters with $PM_{2.5}$ Samplers Shown in Background

Figure 7. Picture Showing 1.8 and 10 Meter Sonic Anemometer and $PM_{2.5}$ Samplers
(Note: Aircraft shown is in a holding area and was too close for effective LIDAR sampling.)

and direction. The average sonic anemometers data were recorded every 10 seconds to a self-contained data logging unit. Data were downloaded, fresh batteries were installed, and maintenance was performed each day before measurements began.

In addition, data from the LLWAS for four stations in the immediate vicinity of the measurements were supplied by the airport, which provided additional wind speed and direction information at additional heights. The LLWAS system is an array of anemometers capable of detecting and/or predicting wind shears occurring at low altitudes in the immediate area.

LIDAR measurements were not performed during precipitation or fog due to the interference of the backscatter on the LIDAR system since backscatter would be greatly influenced leading to errors. The Team experienced rain during the campaign, which resulted in loss of measurement time at location A and prevented the Team from taking measurements at locations B and C that were depicted on Figure 3.

Ambient Particulate Matter Sampling

Ambient $PM_{2.5}$ samplers were used in the vicinity of the OPAL system to establish background levels for fine particulate matter. These samplers, also shown in Figures 6 and 7, collected the $PM_{2.5}$ on filters. Two samplers were employed in the immediate area. One was allowed to run for a full 24-hour period, while the second only collected samples during the hours of LIDAR operation. This permitted a review of the background over a full day and comparison during actual sampling. The samplers were carefully calibrated each day for flow rates of 5 liters/minute and care was taken in handling the filters to avoid contamination. Each filter was contained in a special cassette holder, so no human contact with the actual filter needed to occur. At the end of sampling periods, the filters, still in the cassette holders, were placed in special plastic cases and sent to a certified laboratory for gravimetric and x-ray florescence analysis. Blank filters were also sent to the lab as a quality control measure.

DATA ANALYSIS

The LIDAR data were first screened using initial quality control to remove suspect data based on equipment calibrations and field note reviews. Next, the quality-controlled raw data underwent additional quality control, review and processing by NOAA. These data were compiled into a usable format for analysis. For this measurement campaign, plume characteristics were determined by the use of software specifically written by NOAA to automate data processing. The data processing resulted in multiple mathematical relationships of the data. Appendix A shows a listing of these tabulated parameters with a description of each. The raw data, such as a typical sweep shown in Figure 8, were also processed into a more useable data form as shown graphically in Figure 9. The information presented in Figure 9 represents the concentration gradients of aerosol matter in the aircraft plume. The resulting representations were used to manually compare, using pattern recognition, the plume characteristics such as the extent of the plume limits

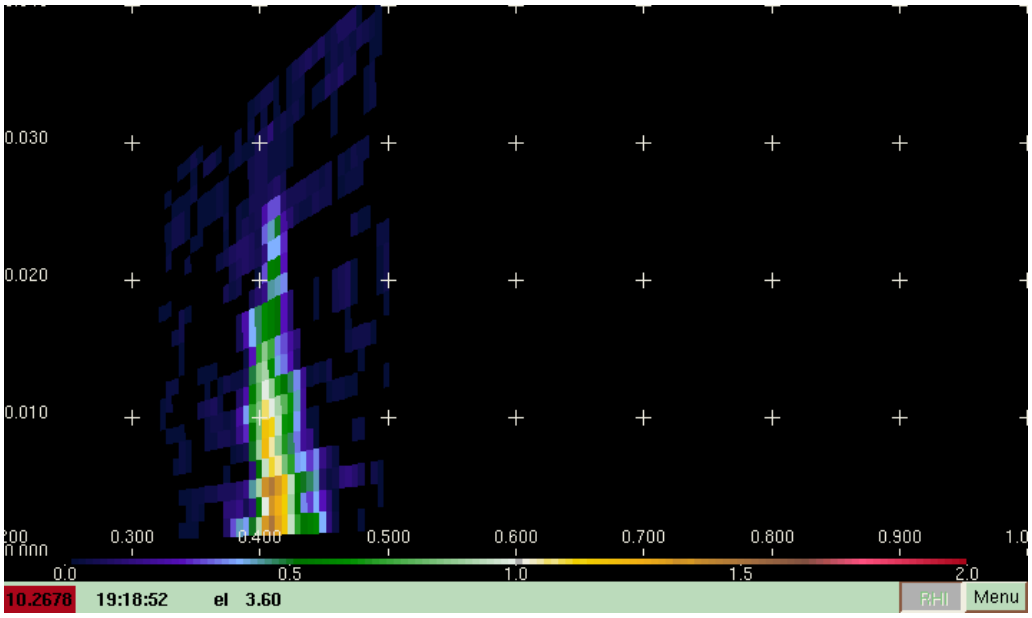

Figure 8. Example Raw Output from the OPAL System

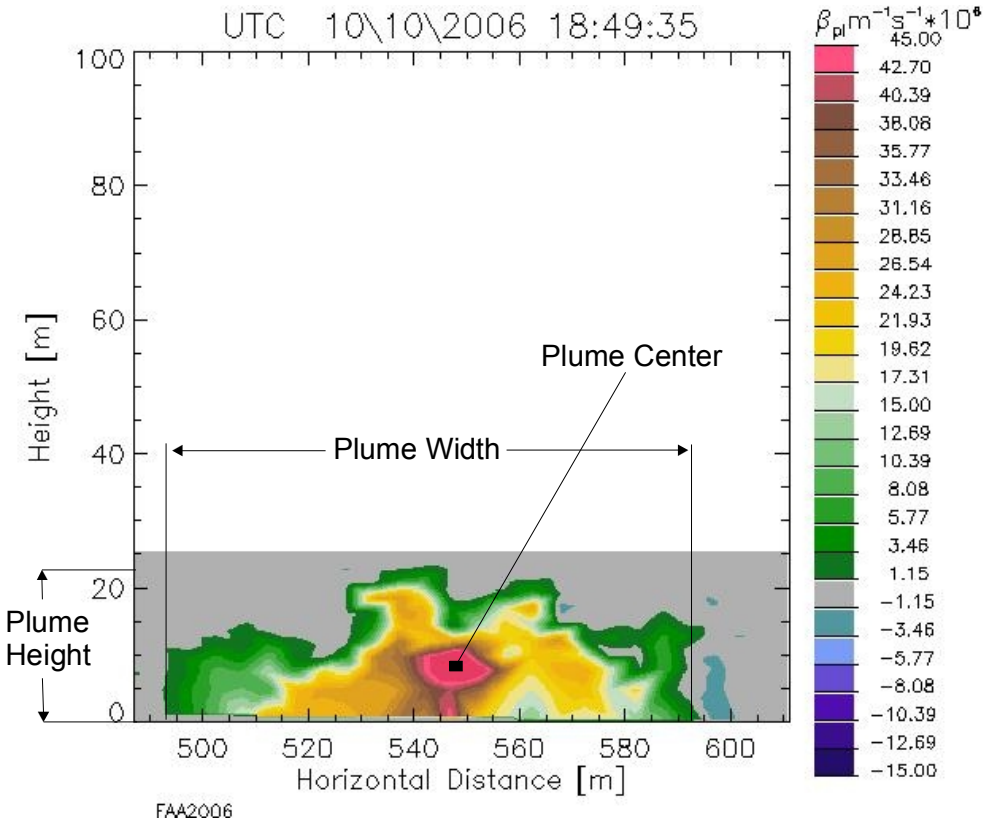

Figure 9. Typical Sweep After Processing

Note: Plume Height as used here is the total vertical dimensions of plume whereas plume rise is the distance from the center of the plume concentration to the ground plane.

and the height at the center of the plume to the automated results from NOAA. Additionally, sweeps in the time series of a scan permitted the changes in plume characteristics to be observed in the cross section to allow a better understanding of the dispersion process.

NOAA formatted the processed data using a commercial spreadsheet to tabulate and review measured parameters, while also combining the data logs, LIDAR results, and measured weather data. NOAA began a more comprehensive review of the data by noting the number of quality sweeps and scans, the number of aircraft and aircraft types measured, and multiple variables related to the key plume parameters. These key plume parameters included the standard deviation of the plume in the vertical (using vertical limits of the sweep), in the horizontal (using horizontal limits of the sweep), and the total height to the center of the plume.

The plume center (Z_{center}) of each sweep was identified, as well as the plume width and the plume height (actual vertical limits of plume). Plume rise (distance from ground plane to the concentration center of the plume) could be determined by observing the changes in the plume center from multiple sweeps for an aircraft takeoff. The Denver data set allowed this analysis (following the plume) to occur for longer times than had been possible for LAX and ATL. The time between each sweep was approximately 4 seconds, which is a slightly faster rate used at ATL but slower than LAX. Following the process used at the two previous airports, each aircraft scan was reviewed and the sweep (cross section) that represented the second highest value for the center of the plume was selected and assumed to represent the plume rise in a conservative fashion. A similarly conservative approach was used to determine the standard deviation of the plume in the horizontal (σ_y) and in the vertical (σ_z), since the same sweep selected for the plume rise determination was used. The selected sweep is the location and size of the plume that is assumed to be the initial plume parameters as it begins to disperse downwind and supplies key input needed to use the Gaussian dispersion modeling approach.

Figure 9 represents a well defined plume. The problems of plume break-up, multiple centers, high plume rise, and irregular shapes led to fragments of the plume being included in many of the derived parameters from the automatic software, which resulted in differences with the manual pattern recognition and the computer processed data. For these reasons, it was not easy to determine the center and fringes of the plume for all sweeps, which led to differences in the computer evaluation as compared to the human recognition method. In efforts to minimize this source of error, a large number of variables were calculated in the automated process by NOAA (see Appendix A). It was found that for the standard deviation in the horizontal, the derived parameter d_{hor} (signal-weighted absolute deviation in the horizontal about x_{median}) and for the standard deviation in the vertical, d_{ver} (signal-weighted absolute deviation in the vertical about z_{median}) provided the best results when compared to the human recognition method. This is consistent with the finding from the ATL study. As such, d_{hor}, d_{ver} and z_{median} were used to estimate the plume for the determination of the horizontal standard deviation (σ_y), vertical standard deviation (σ_z), and plume rise, respectively.

For the four days of in-situ measurements, a total of 511 aircraft takeoff events of 29 different types of aircraft were included in the final data set. This resulted in 5542 sweeps being used in the final analysis for the full data set and 508 sweeps in the second highest plume rise analysis.

Plume Characterization

Using the selected parameters from the LIDAR data, plume parameters were computed for each day and averaged over the sample period. The results of this analysis are shown in Table 1. The average reported value for all three days is not a weighted average but rather an average by day. Average by day values were chosen because the authors think the changes in weather conditions day to day are more important than the number of samples taken in any given day. The data are shown by day as a complete data set and as a sub-set consisting only of the second highest plume rise. As previously discussed, the second highest plume rise sweep for each scan was selected to represent plume rise. As such, while the total data have been shown in Table 1 for comparative purposes, the discussion will be limited to the second highest plume rise data set in the analysis.

Table 1. DEN Final Plume Characterization Derived Parameters

Date	Total # of Aircraft Scanned	Total # of Aircraft Types Scanned	Total # of Scans	Derived Parameters (meters)					
				Full Data Set			2nd Highest Plume Center Data Set		
				σ_y	σ_z	Plume Rise	σ_y	σ_z	Plume Rise
10 Oct	116	23	1340	17.0	5.5	10.9	18.1	6.6	13.3
11 Oct	167	21	1785	14.3	4.7	9.3	14.4	5.6	11.3
12 Oct	159	23	1709	16.3	5.4	10.6	15.9	5.9	12.1
13 Oct	69	11	708	15.0	5.0	10.0	15.1	5.8	11.8
Averages of All Three Days				**15.7**	**5.2**	**10.2**	**15.9**	**6.0**	**12.1**

From the sampling at each airport, average values have been derived for plume rise, horizontal standard deviation and vertical standard deviation. These variables were then compared airport-to-airport. Currently we have data from and can compare three airports (3 values for each variable). While there are too few data to determine a meaningful variance, it can be determined from the three columns on the right in Table 1 that the range of values are 3.8 m for σ_y, 1.9 m for σ_z, and 4.0 m for plume rise when all days are

compared. These values are, in general, small compared to the absolute values, which provide a greater measure of confidence in the average values.

The comparison of the overall values derived during the previous sampling at LAX and ATL are shown in Table 2. Of note is that the average values are close to those values derived from LAX now used in EDMS (values now used are 12.0, 10.5, 4.1 for plume rise, σ_y, and σ_z, respectively). The averages could be applied to update EDMS and a measure of uncertainty can finally be established as one-half of the range. More data will continue to make these values more accurate and allow for a greater evaluation of uncertainty.

Table 2. Comparison of Overall Plume Parameters for All Three Airports (meters)

	LAX	ATL	DEN	AVG	RANGE
Plume Rise	12.0	8.4	12.1	10.8	3.7
σ_y	10.5	11.2	15.9	12.5	5.4
σ_z	4.1	4.3	6.0	4.8	1.9

Aircraft Type Trends

Results from LAX and ATL seemed to indicate a difference based on the type of aircraft, especially due to the location of the engine mounting. Aircraft measurements at DEN were divided into the same three groupings as at the two previous airports: wing mounted engines, fuselage mounted engines, and commuter aircraft. Table 3 shows the results based on aircraft type for the three plume parameters for this analysis.

Table 3. Aircraft Type Analysis Results for Airfield Measurements at DEN

	Wing Mounted			**Fuselage Mounted**			**Commuter**		
Date	Plume Rise (m)	σ_y (m)	σ_z (m)	Plume Rise (m)	σ_y (m)	σ_z (m)	Plume Rise (m)	σ_y (m)	σ_z (m)
Oct 10	12.3	19.3	6.2	15.7	16.3	7.2	7.4	11.8	3.4
Oct 11	11.5	15.1	6.0	12.4	11.8	5.9	4.9	9.6	2.1
Oct 12	11.8	17.6	6.0	14.4	12.9	6.6	4.9	9.4	2.1
Oct 13	13.4	17.4	6.4	7.8	7.4	3.3	4.3	10.3	1.4
Average	**12.3**	**17.4**	**6.2**	**12.6**	**12.1**	**5.8**	**5.4**	**10.3**	**2.3**

In the comparison of aircraft types, it can be seen that the range of values is sometimes less and sometimes greater in relation to the ranges indicated in Table 1. The wing mounted and commuter ranges are all smaller except for σ_y and σ_z, respectively. For the fuselage mounted aircraft, all ranges are greater, indicating increased uncertainty for this aircraft type. However, the ranges for all aircraft types are still less than the overall averages and as such are still considered representative of the data.

As noted by the yellow highlighted cells, some days (temporal data) seem to vary more from the average than others. However, the same trend did not extend for all aircraft types on any one day. It can be concluded that variables other than meteorology must be considered, since changes in dispersion parameters generated by weather conditions would have been the same for all aircraft types on any particular day.

Exploring this idea, the fuselage mounted aircraft on October 13 seems to offer the most hope to discover any trend in variability and the mix of fuselage mounted aircraft for October 13th was examined more completely. It was found that there were 7 scans of larger (e.g., MD80) fuselage mounted aircraft on the first two days and 11 on the third day, but no events occurred on October 13th. Including the smaller fuselage mounted aircraft that carry 80 passengers or more, there were 23 events on the 10th, 26 on the 11th, and 30 on the 12th, but only 4 on the 13th. The small sample on October 13th does not seem representative of daily fuselage mounted aircraft flights and consideration was given to ignoring this data and effect on overall results. If these values are not used, the final parameters for fuselage mounted aircraft would be 14.2, 13.7, and 6.6 meters for plume rise, σ_y and σ_z, respectively. This represents an increase in all three parameters. Perhaps more importantly, it seems to indicate that aircraft may also need to be characterized by size or thrust as well.

Next, the trends were compared with those of LAX and ATL, as shown in Table 4. The largest differences from average are highlighted. It can be seen that even though there is still variance among the data, the ranges are still small compared with the average, so averages may provide reasonable quantification of the parameters.

Table 4. Comparison of Derived Dispersion Parameters from 3 LIDAR Measurement Campaigns

Parameter	Aircraft Type	LAX	ATL	DEN	AVG.
Plume Rise (m)	Wing Mount	11.1	7.9	12.3	10.4
	Fuselage Mount	14.6	11.4	12.6	12.9
	Commuter	12.1	5.3	5.4	7.6
σ_y (m)	Wing Mount	11.0	13.3	17.4	13.9
	Fuselage Mount	10.0	13.2	12.1	11.8
	Commuter	10.3	8.1	10.3	9.6
σ_z (m)	Wing Mount	3.8	4.0	6.2	4.7
	Fuselage Mount	4.8	5.9	5.8	5.5
	Commuter	4.1	2.8	2.3	3.1

Trends in aircraft type seem to occur at all airports. However, with the limited data and the associated ranges of data, it is not conclusive that separate estimate values should be used for wing mounted versus fuselage mounted aircraft. This leads to a conservative approach of one set of values for both wing and fuselage mounted aircraft even though the overall uncertainty for any discrete event will increase. A better case can be made to use a separate value for the commuter aircraft, but distributions still overlap, indicating that no discrete data populations for the commuter aircraft type can be absolutely proven statistically. This is illustrated in Figures 10, 11 and 12. In these three figures, the range for each of the three parameters is illustrated on the right next to the overall averages to allow a visual comparison of the ranges and averages. Also included are the individual averages from each airport, shown as discrete data points.

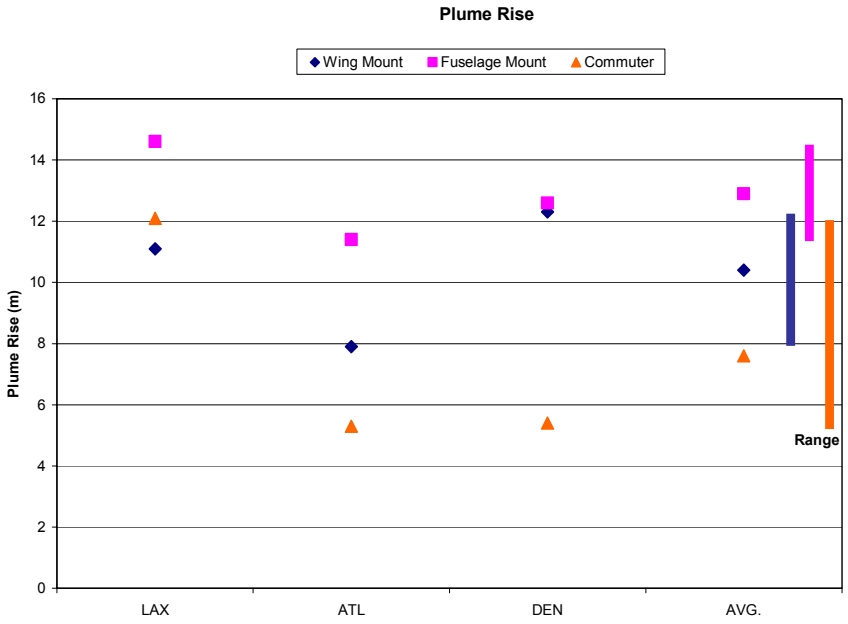

Figure 10. Comparison of Plume Rise for All Airports

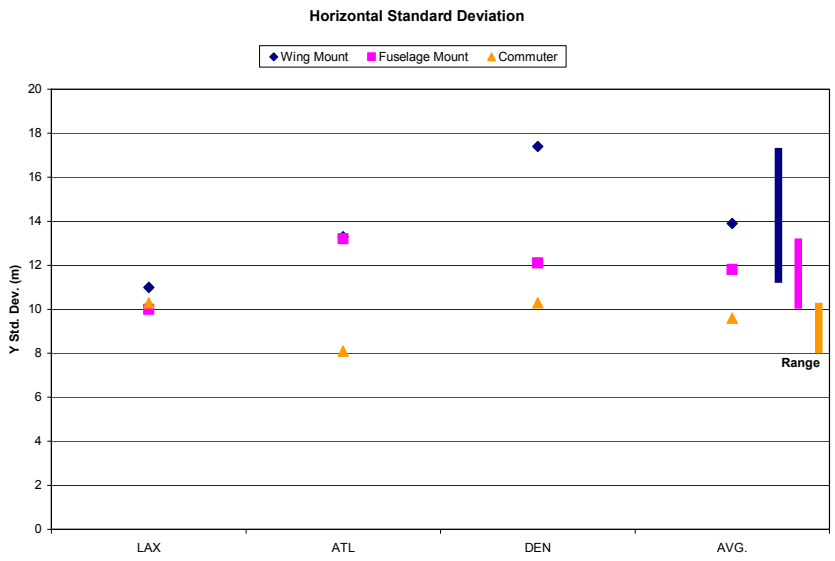

Figure 11. Comparison of σ_y for All Airports

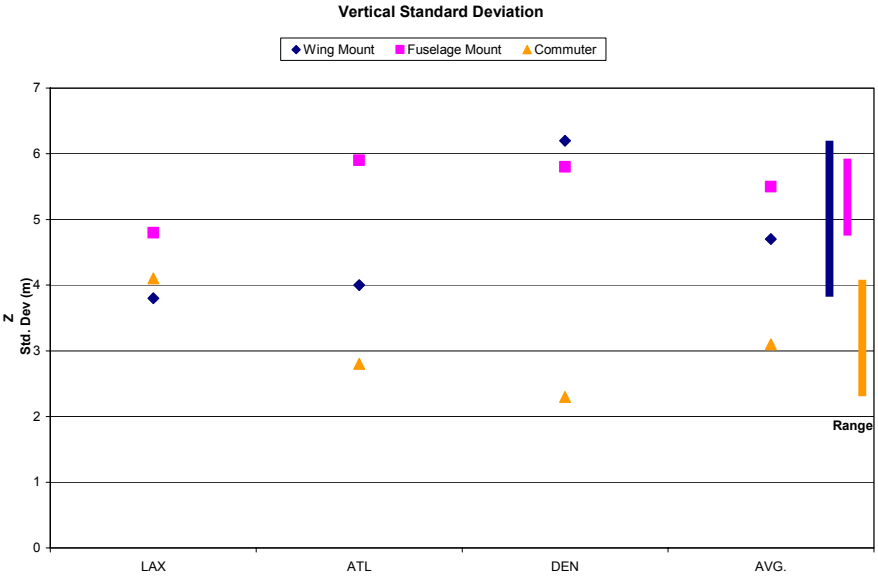

Figure 12. Comparison of σ_z for All Airports

Statistical Testing of Airfield Data for Changes Due to Weather

Data were analyzed to see if trends existed for key weather parameters (temperature, wind speed, wind shear, and wind direction). This was done by statistical testing of the data was also used to determine if variance in the weather or the type of aircraft resulted

in correlated changes with the determined plume parameters. The meteorological data used during comparisons for correlation with the LIDAR measured data included:

- Sonic anemometers at 1.8 and 10 meters (wind speed and direction)
- Wind vane at 7.5 meters
- Cup anemometer at 7.5 meters
- Temperature at 7.5 meters
- Low Level Windshear Alert System (LLWAS) at 30 meters (2 stations), 15 meters and 12 meters

As described in previous reports[1,2], plume rise and plume spread may be influenced by local meteorological variables such as temperature, wind speed, wind direction, and turbulence. The temperature difference between the ambient air and the jet exhaust provide thermal buoyancy that leads to both plume rise and vertical dispersion. The wind speed acts against this vertical motion and may cause the plume rise and vertical plume spread to be reduced. The wind direction could have an effect on the initial parameters if wind is blowing across the runway as compared to along the runway within allowable ranges due to safety[5]. Unfortunately, in the previous studies, meteorology data were lacking to provide a detailed analysis and no findings were forthcoming. For the DEN measurements, more detailed weather information was available to allow a more in depth analysis of effects on derived plume parameters than for LAX and ATL.

Temperature Effects

In the previous two studies, plume rise was analyzed according to the generic equation shown as Equation 1.[6]

$$\Delta h(x) = \text{constant } (Q_h)^a (x)^b (u)^c \qquad [1]$$

where:

$\Delta h(x)$ = plume rise as a function downwind
Q_h = heat emission rate
x = distance downwind
u = wind speed at source height
a,b,c = constants

No correlation was found between wind speed, wind direction, and the derived plume parameters in previous reports based on the limit meteorology data available. The final conclusion was that Equation 1 could be reduced to a function which was completely based on the heat emission rate relating to thermal buoyancy as shown in Equation 2:

[5] http://www.faa.gov/airports_airtraffic/airports/resources/advisory_circulars/media/150-5300-13/150_5300_13_part2.pdf

[6] Reviews of this material can be found in:
Stern, A.C. Ed., Air Pollution, 3rd Edition, Volume I, Academic Press, New York, 1976.
Zannetti, P., Air Pollution Modeling, Bookcraft Ltd, Avon, U.K., 1990.

$$\Delta h(x) = \text{constant } (Q_h)^a \qquad [2]$$

This implies that the high temperature of the jet turbine exhaust, resulting in a stong heat flux parameter, is the dominant reason for the plume rise. This finding was checked again with DEN data by comparing ambient temperature to the derived plume parameters as mixed pairs. Figure 13 is a typical scattergram of the data comparison. As can be seen, very little correlation existed for ambient temperature changes and the three plume parameters. The correlations were R^2 values of 0.035, 0.0622, and 0.0371 for the comparison of ambient temperature to plume rise, σ_y and σ_z, respectively. The resulting correlation coefficient and linear trend lines for each comparison are included. As in the previous two studies, no significant correlation was shown.

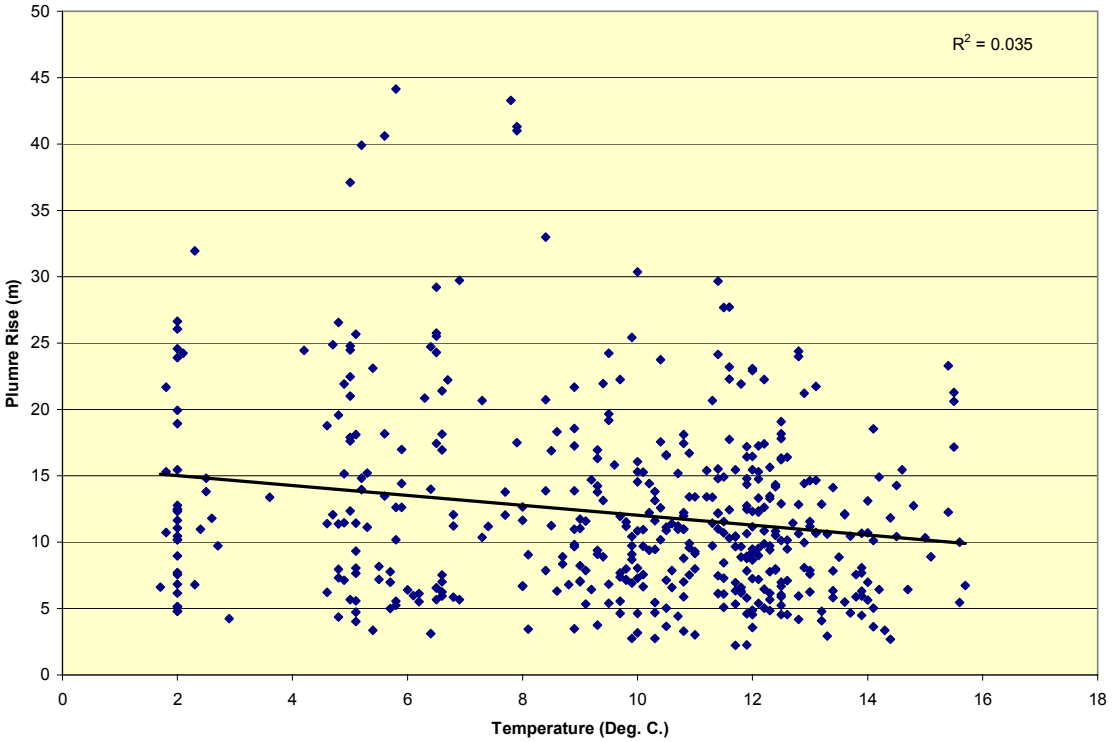

Figure 13. Scattergram of Plume Rise and Ambient Temperature (correlation poor)

Wind Speed Effects

Efforts were taken to gather higher resolution wind speed information than what was available for the previous two studies. Figure 14 shows a comparison of the different equipment and different heights used to measure wind speeds. Data points indicate short

term time averages. As expected, the data compare well, indicating proper operation and reporting from all sources.

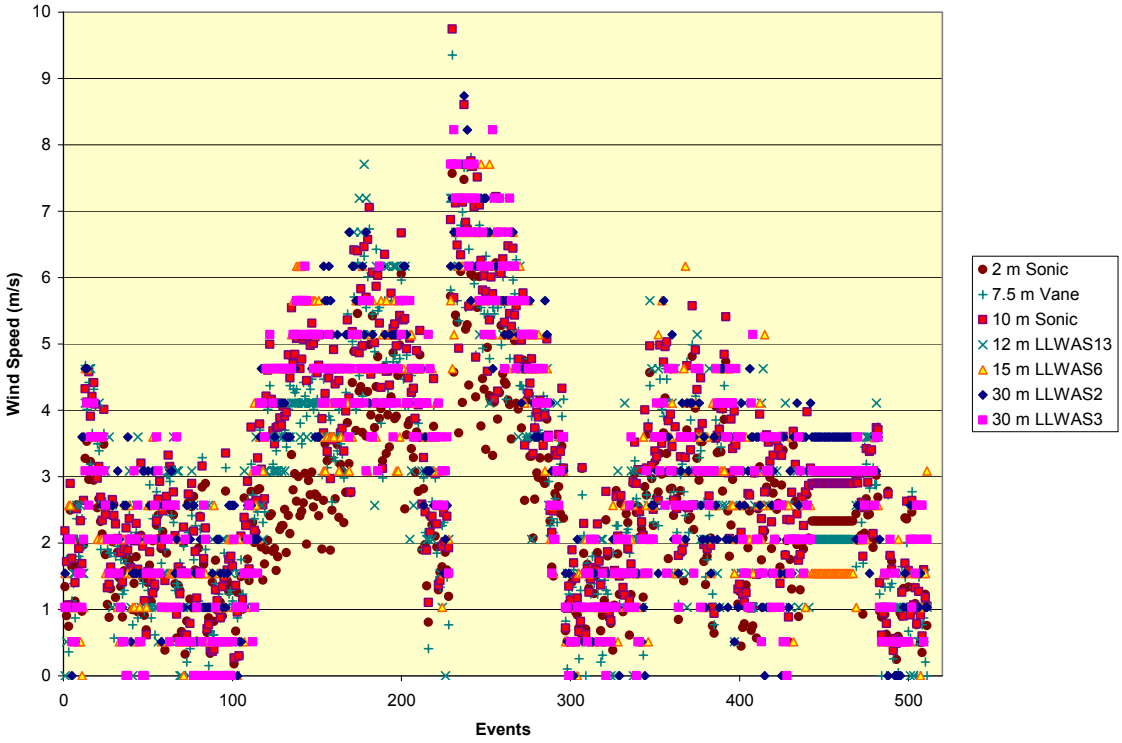

Figure 14. Comparison of Wind Speeds from the Various Equipment

Wind speed effects add a vector consideration to the wind, so the derived plume parameters were evaluated to see if there was a correlation with wind speed. Very poor correlation was found when comparing average wind speed at 10 meters to the three plume parameters which mirrors the results at previous airports. A typical scattergram comparing wind speed to the plume rise is shown in Figure 15 as an example of the poor results. R^2 values were 0.001, 0.0155, 0.0005 for the plume rise, σ_y and σ_z, respectively. As before, only one scattergram is shown for brevity.

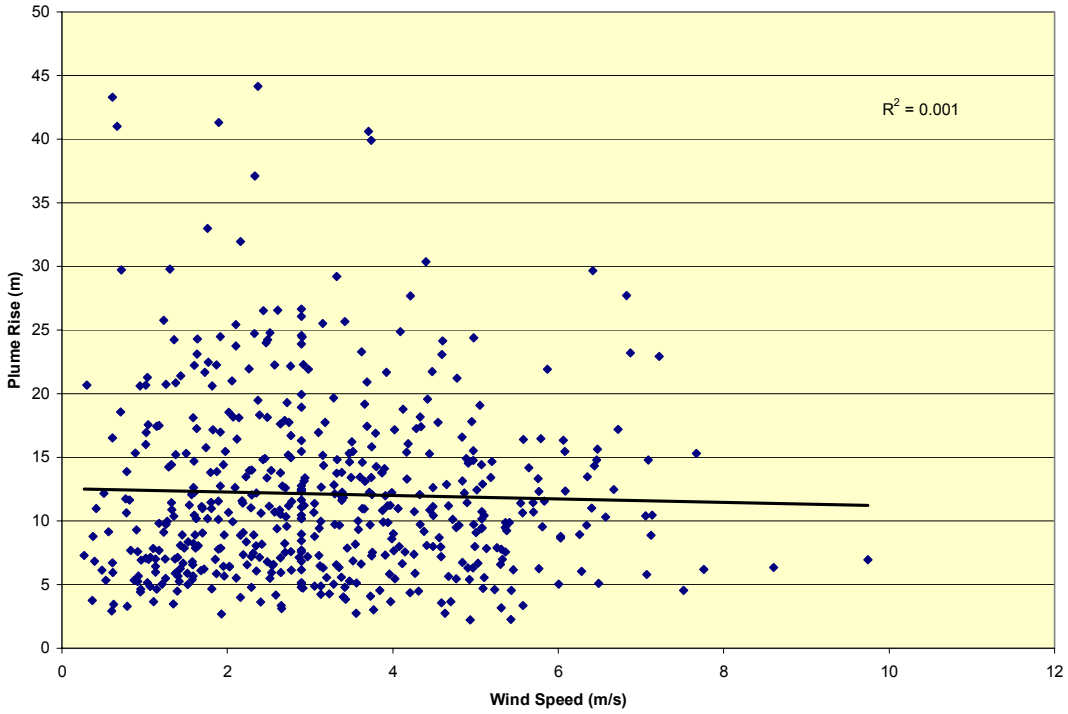

Figure 15. Scattergram of Wind Speed Compared to Plume Rise (correlation poor)

However, this data set taken at DEN, had measured values at multiple heights locally, permitted a more in depth analysis of the changes in wind with elevation or vertical wind shear[7].

Wind Shear Effects

No significant correlation was shown when the wind shear from the 3-D sonic anemometers at 1.8 and 10 meters when compared to the plume rise. Wind shear with different combinations of elevation were then analyzed. A definite pattern was shown when the wind shear was compared to plume rise using the 12 and 30 meter heights of the LLWAS. As the analysis continued, the data were segregated into positive shear (wind speed increasing with height), negative shear (wind speed decreasing with height), and the no shear condition (wind speed the same at both heights). Figure 16 shows these results. While the correlation coefficient is not extremely high, it does show what the team feels are important trends. The trend lines show a decreasing trend for negative shear and an increasing trend for positive shear. Near the no shear condition, it is also interesting to note that the scatter in the data becomes much larger.

[7] Wind shear is the change in wind speed over a relatively short distance in the atmosphere. Vertical wind shear, used in this document is the change in wind speed with height.

The first conclusion that can be made is that while the vertical wind shear closer to the ground (1.8 to 10 meters) did not indicate a significant effect on plume rise, the shear at a greater height (12 to 30 meters) indicated a much stronger correlation and hence a significant effect. Both comparisons had a separation of 8 meters but with much different results. This may be explained by the location the wind shear was measured. The derived plume rise of 12 meters, at the height of the lower LLWAS sensor, is in the range of the LLWAS wind shear and appears to have a direct effect on the plume rise. This is reinforced from the analysis of the wind shear from 1.8 to 30 meters, as shown in Figure 17. The correlation coefficients, while still showing a degree of correlation, have dramatically decreased when a greater range of heights away from the plume center were compared. Also, if the range of 15 to 30 meters is used from the LLWAS data, the correlation is still less than for 12 to 30 meters (see Figure 18). Other ranges were also evaluated but did not show a similar degree of correlation as the 12 to 30 meter analysis.

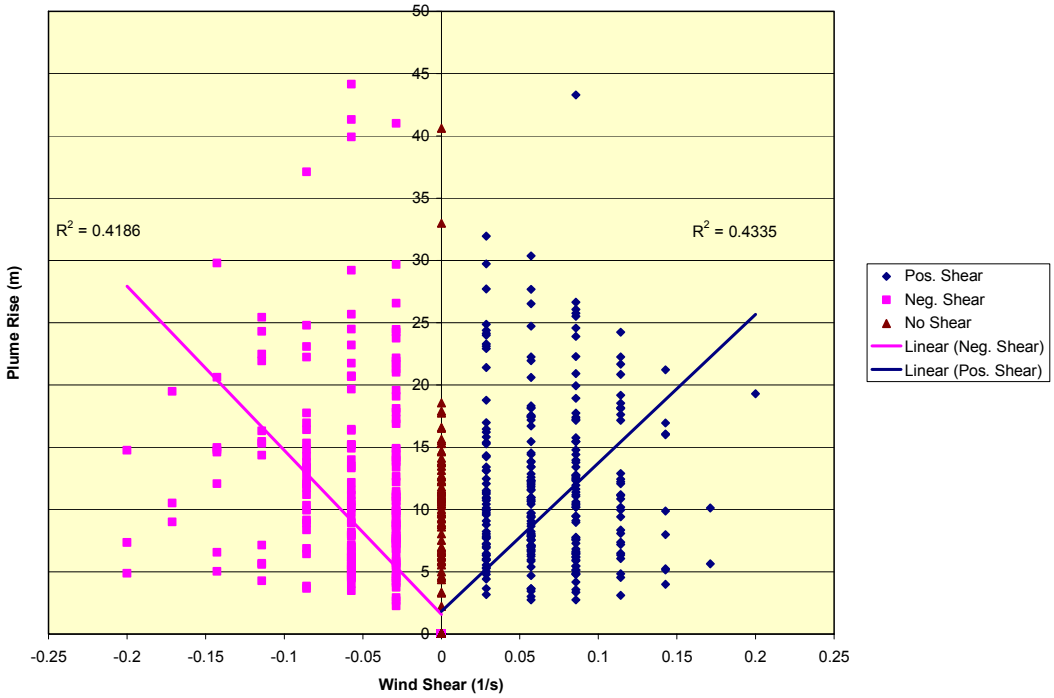

Figure 16. Comparison of Wind Shear from LLWAS (12 and 30 meters) to Plume Rise

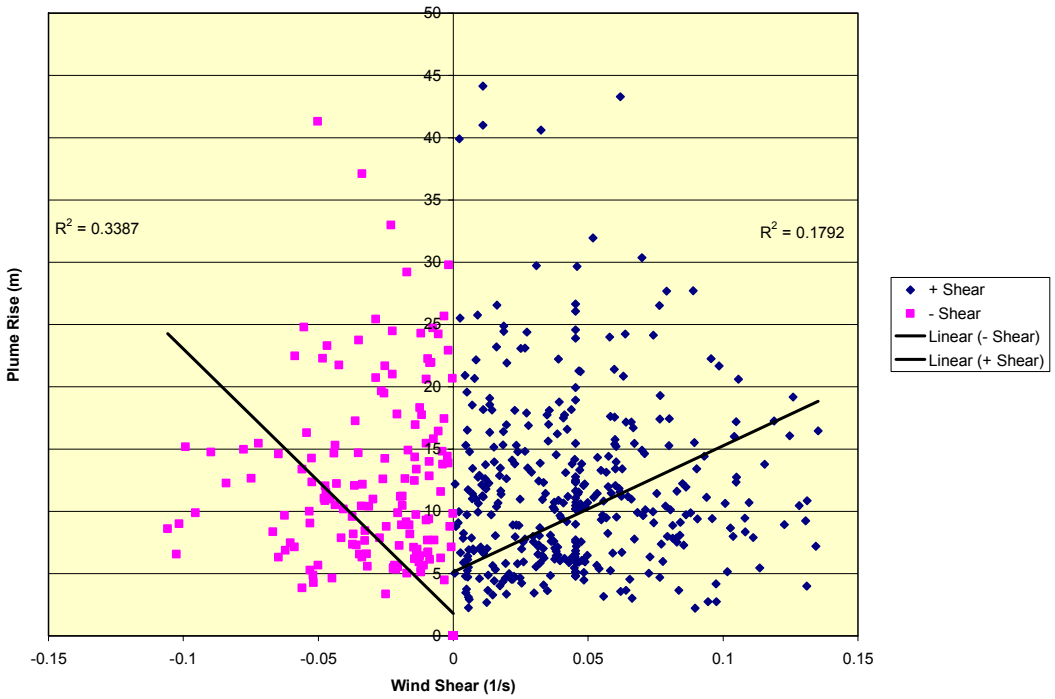

Figure 17. Comparison of Wind Shear from Sonic 3-D and LLWAS (1.8 and 30 meters) to Plume Rise

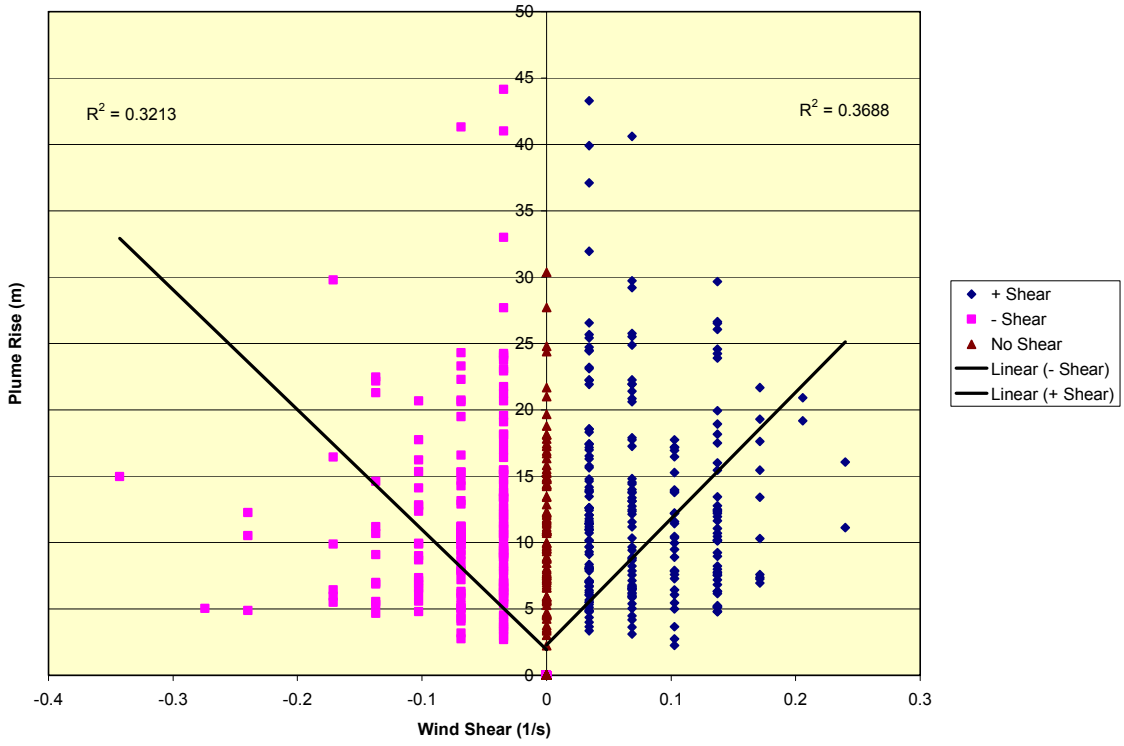

Figure 18. Comparison of Wind Shear from LLWAS (15 and 30 meters) to Plume Rise

A further test was performed to determine the correlation between the wind speed from the 12 meter LLWAS and the derived plume rise, which is also 12 meters on average. No significant correlation was shown ($R^2 = 0.0002$). The final conclusion that can be drawn is that it is extremely important that in future measurements the wind shear be measured in the ranges of the expected plume height. This could be done by both experimental design and the use of LLWAS data.

It is also important to note that at first glance, Figure 16 is slightly misleading. The greatest plume rise values occur as the wind shear approaches zero, but the trend is a decreasing plume rise with increasing vertical wind shear. This is because two forces are having an antagonistic effect. It is concluded that thermal buoyancy appears to result in the greatest plume height when there is no wind shear and the vertical forces are dominant. As the wind shear increases, the horizontal forces increase and the plume cannot rise as efficiently as in the no shear case. This results in the plume being held closer to the ground. However, as wind shear increases further, the atmosphere becomes more unstable and wind shear begins to induce vertical movement into the plume. This results in the plume height increasing with increased wind shear. In an effort to quantify this effect, the data were analyzed using the following common approach:

$$u_2/u_1 = (h_2/h_1)^n \qquad [3]$$

Where:
u_2 = wind velocity at height 2
u_1 = wind velocity at height 1
h_2 = height 2
h_1 = height 1
n = exponent allowing stability class to be defined

This method, used in the EPA Climatological Dispersion Model[8] allows stability to be evaluated with values of n being put forward by multiple researchers for different surface roughness such as DeMarriais[9] and Davenport[10]. While the derived n values were in the ranges expected, no correlation to the plume rise was shown with the R^2 values being only 0.001. So, while the trends are thought to occur as previously explained, the reason for the overall trend was not proven from this analysis of the stability parameter.

Unfortunately, temperature differentials with height were not measured because of the need for a larger tower which was thought to be intrusive and perhaps a safety concern. However, since the lapse rate[11] also plays such an important part in the measurement of turbulence and subsequent dispersion, it would follow that this parameter would also be extremely important. This indicates the need in future testing to also measure

[8] Environmental Protection Agency, "User's guide for the Climatological Dispersion Model", U.S. EPA Publication EPA-R4-73-024, December, 1973.
[9] DeMarrais, G.A., "Wind speed profiles at Brookhaven National Laboratory", J. Applied Meteorology, 16:181, 1959.
[10] Davenport, A.G., "The relationship of wind structure to wind loadings", International Conf. on the Wind Effects on Buildings and Structures, National Physical Laboratory, England, June, 1963.
[11] Lapse rate is the change in atmospheric temperature with height.

temperature at two heights so that lapse rate can be determined and other analyses such as the Richardson Number[12] could be evaluated. An alternative that could also be used would be to measure the vertical heat flux to infer stability. This would permit a better understanding of the turbulence for subsequent measurement opportunities. The best way to accomplish these measurements will be reviewed prior to any future measurements.

Wind Direction Effects.

Figure 19 shows a comparison from all measurement stations, again showing similar trends, leading to confidence in the measured data. For completeness, wind direction was also compared with the three plume parameters. Figure 20 shows a typical scattergram from this analysis. No significant correlation was shown between wind direction and the plume parameters as illustrated in Figure 20. However, to follow up on this analysis with the additional data available from this study, the change in wind direction with height[13] was also evaluated. The depth to which the Ekman spiral penetrates is determined by how far turbulent mixing can penetrate, and relates to the frictional characteristics of the surface. The change in wind direction with height from 12 to 30 meters, where the effect of wind shear was shown, was compared to plume rise. Unfortunately, no statistical significance was shown, even though the data were analyzed in multiple ways. As such, wind direction is not seen as a major variable in plume rise.

Continuing Turbulence Analysis

NOAA and Volpe are continuing to work together to analyze information from Denver and from the other airports that have been sampled. This information will be contained in a separate, stand-alone report with recommendations for any future campaigns**.**

CONCLUSIONS

All three airport studies have successfully resulted in LIDAR response cross-sections of the aircraft jet turbine exhaust plume during takeoff roll. The DEN study offers additional insights into aircraft plume behavior, and data for more accurate modeling of plume rise and spread. Added to the LAX and ATL results, it provides a more robust data set.

In general the DEN results tend to validate the previous findings although individual difference airport-to-airport occurred. It is still obvious that substantial plume rise occurs and that initial plume spread is also evident. To fully quantify plume rise and plume spread in a generic fashion for use at any airport more measurements at additional airports are needed to continue to reduce site bias and allow valid statistical results.

[12] The Richardson number, named after Lewis Fry Richardson (1881 - 1953), is the dimensionless number that expresses the ratio of potential to kinetic energy.

[13] The Ekman spiral is a phenomenon where the wind direction near a horizontal boundary (in this case the ground) rotates as one moves away from the boundary.

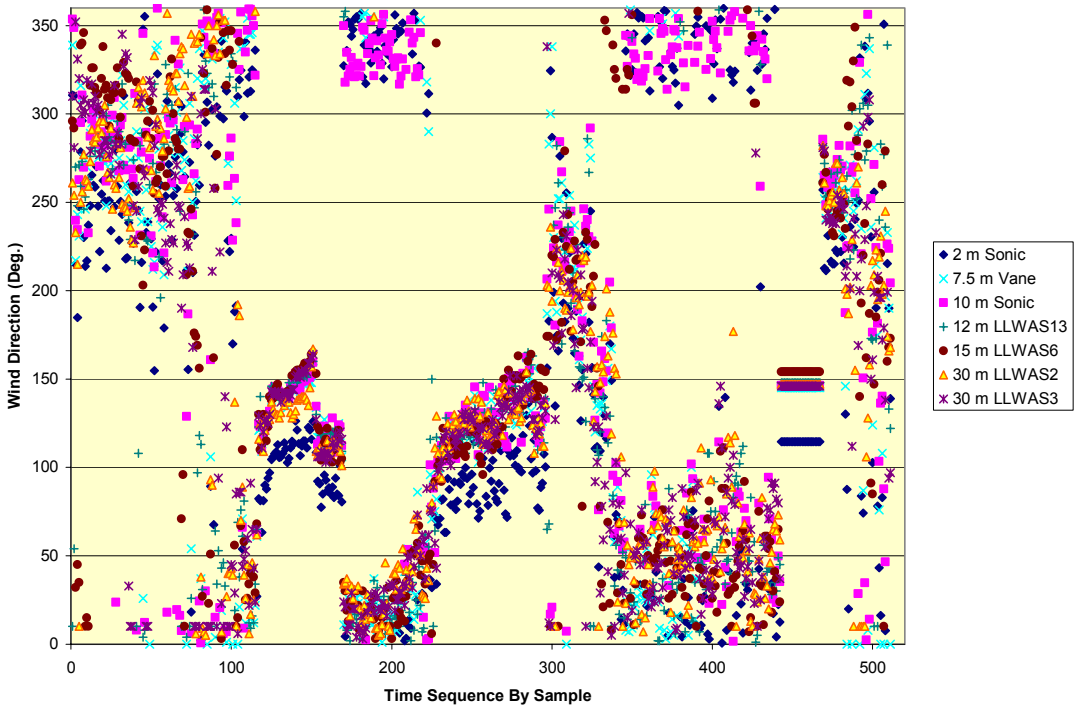

Figure 19. Comparison of Wind Direction from All Measurement Stations

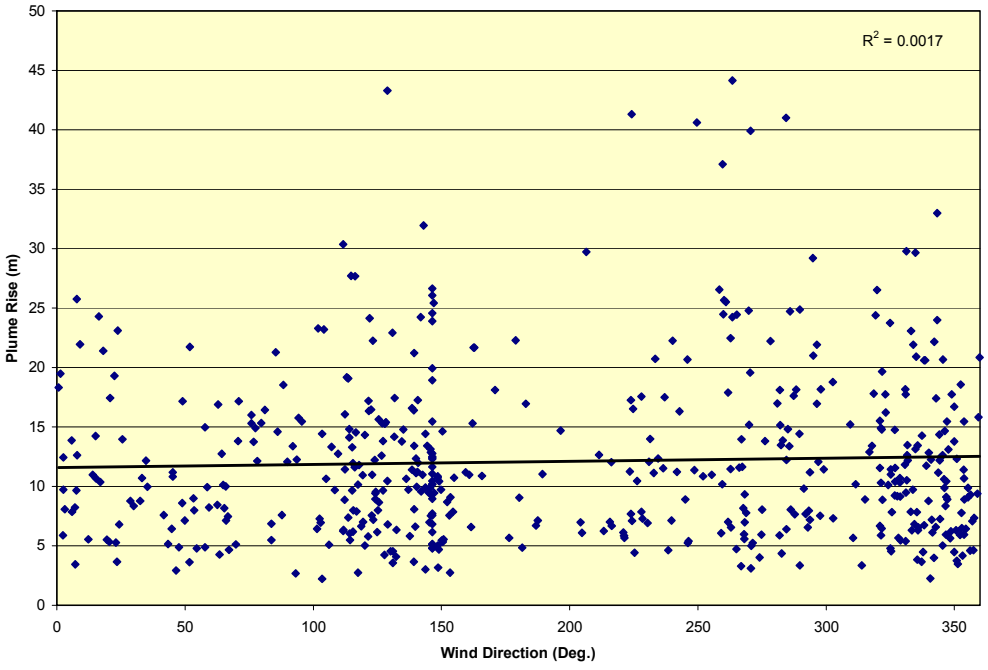

Figure 20. Demonstration of no correlation between Wind Direction and Plume Rise

Resulting generic values would improve the prediction results of dispersion models used for NEPA analysis, exposure quantification, and evaluation of health effects.

Values now in use come from the LAX measurements. It is concluded by the Team that use of the average values from all three airports, including a degree of uncertainty by including one-half of the derived ranges, would lead to more accurate dispersion analysis for any given airport as site bias is reduced. These values are:

Values now in use (from LAX):

- Plume Rise: 12.0 meters
- σ_y: 10.5 meters
- σ_z: 4.1 meters

Recommended replacement values (from all three airports):

- Plume Rise: 10.8 ± 1.9 meters
- σ_y: 12.5 ± 2.7 meters
- σ_z: 4.8 ± 1.0 meters

The changes in standard deviation would result in over a 39 percent increase in plume area at the initial modeling point. Since plume spread and concentration estimates are inversely proportional in the result from these parameters would be a lower predicted concentration. Of course with distance the difference would become smaller but the new parameters would always result in lower concentrations. However, the smaller plume rise, combined with a greater σ_z would increase ground level concentration (defined as 1.6 meters above the ground) at the initial modeling point. Downwind the differences would be less but concentrations would always be greater in flat terrain. The overall effect, in the near field, would be to increase predicted concentrations but detailed modeling is needed to truly evaluate the effects, especially at greater distances.

The exception to this recommendation of the values combined from all three airports are the airports where testing has occurred. It is recommended that these airports use the actual values derived for their own airports as reported in Table 2.

The DEN measurements have also advanced the idea of separating aircraft based on airframe and engine differences. If these values are assumed to be independent variables and used during the dispersion process (e.g., EDMS), the dispersion estimates could be more accurate. In terms of engine mount location and larger aircraft vs. commuters, it was shown that the distributions appear to be separate but overlap. As such, it cannot statistically be proven that these are independent categories but it appears very likely. While the Team would recommend that caution be applied and that more data is really needed before this can be absolutely proven by the use of statistics, the values derived by from the measurements taken to date would be:

Wing Mounted Large Commercial Aircraft

- Plume Rise: 10.4 meters
- σ_y: 13.9 meters
- σ_z: 4.7 meters

Fuselage Mounted Large Commercial Aircraft

- Plume Rise: 12.9 meters
- σ_y: 11.8 meters
- σ_z: 5.5 meters

Commuter Aircraft

- Plume Rise: 7.6 meters
- σ_y: 9.6 meters
- σ_z: 3.1 meters

The analysis for meteorological impacts was advanced in the DEN measurements since more meteorological data were available for this measurement campaign than in previous measurements. Wind shear at the plume rise height was shown to be important to the plume rise. Poor correlation was found with temperature, wind speed and direction when directly compared to plume rise. On the other hand, the success of the wind shear analysis suggests that additional information would provide for a more in depth analysis and a better theoretical understanding of the plume dynamics. This also suggests that not only the need for wind speed measurements at multiple heights in future measurements, but also that there is a need for the measurement of lapse rate in the immediate vicinity to allow a more complete analysis.

These results again indicated that thermal buoyancy is a critical factor in plume rise. With no wind shear, the highest plumes occur and are assumed to do so due to thermal buoyancy providing the vertical movement and no conflicting vector forces on the plume. However, as wind shear begins, the horizontal component of the forces tends to hold the plume closer to the ground. Then as wind shear continues to increase, indicating decreased stability in the atmosphere, vertical movement is enhanced and the plume rise begins to increase once again.

To advance the hypotheses presented in this report, more testing is needed at other airports and changes to the collection methodology as well as additional work have been identified. These include:

- Direct determination of atmospheric stability, either by temperature at two heights with precision, aspirated thermometers along with wind speed, or a ambient vertical heat flux and wind measurement.

- Continue exploring trends of different aircraft engine mount locations and the effects on exhaust plume size and plume rise through additional measurements.
- The data tends to indicate that the dispersion parameters from commuter jet aircraft could be modeled independently because of the difference in spread and plume rise, although it cannot be absolutely proved statistically at this time. Additional testing could provide the information for a decision that could be backed by statistical analysis.
- Division of the commuter class into a large (over a specific number of seats) and small (under the same specific number of seats) for continued analysis of future data and retro analysis of the existing data.
- Separation of the fuselage mounted aircraft into more specific categories based on size such as small commuter, large commuter, and large commercial jetliner.
- Evaluation of the plume rise by aircraft type based on the exhaust heat flux for future measurements and retro analysis of existing data. This would require using existing data in a meaningful way. Initial thoughts include the use of a mixed variable from the thrust and fuel flow parameters found in the ICAO Databank.

Each data set has added to the body of knowledge and improved the understanding of the characteristics of plumes emitted by jet turbine aircraft. But variations in the data continue, leading to uncertainty unless these can be quantified and tied to local variables. Additional measurements will continue to reduce this uncertainty, and lessons learned from previous measurement campaigns have improved each subsequent campaign. Theory will continue to be employed to quantify differences. The research from the three airports has dramatically increased our understanding of the correct sampling methods (both LIDAR and local variables) and our understanding of plume behavior. The benefits of remote sampling of jet aircraft emissions have yet to be fully realized, but offers a relatively low cost alternative to the measurement of aerosols from aircraft and should also be pursued.

FUTURE WORK

The data from all three airports for the in-situ airfield measurements should be combined into a single, more robust database. Sensitivity studies could be performed on EDMS using the EPA's AERMOD Gaussian dispersion model, incorporating the findings of each of the three airports, as well as a verification using the combined airports database if measurement data were available. However, while having data from three locations is better than anything to date, it most likely still includes site bias since only three, very different, airports have been measured and each displayed overall differences in the data.

The Team concludes that additional studies should be carried out to evaluate potential changes in the derived parameters to reduce the error due to site characteristics (site bias). Additional studies would continue to expand the database and improve the derived

parameters for plume characteristics (plume rise and initial plume spread). These follow-on studies will be important to:

- Allow further exploration of plume rise variables and confirm that the exhaust gas temperature may be directly correlated.
- Provide a more extensive data set to allow the analysis of the effects of aircraft types and atmospheric stability to be more accurately defined.
- Allow the inclusion of more detailed meteorological data such as lapse rate in the immediate vicinity of the testing.
- Allow for continued development of remote sensing of mass in future sampling

APPENDIX A

LISTING OF LIDAR VARIABLES

Table A.1. Reported LIDAR Data Parameter Description

Parameter	Units	Description of Parameter
day	(UTC)	Day of month sweep started
month	(UTC)	Month of Testing
year	(UTC)	Year of Testing
start hour	(UTC)	Decimal time sweep started: for example, 21.5000 = 9:30 pm
end hour	(UTC)	Decimal time sweep ended
Event #		Sequential numbering assigned during measurement of aircraft events to assist in later data reduction
tail number		Aircraft tail number from spotter and/or departure log
A/C		ICAO code for aircraft type
AL		IATA code for airline
Sweep Dir		-1 = up, 1 = down
Ny		Number of horiz elements in gridded data array
y0	m	horiz dist from lidar to nearest grid point in data array
Δy	m	horiz spacing of grid points in data array
Nz		Number of vert elements in gridded data array
z0	m	vert dist from lidar to nearest grid point in data array
Δz	m	vert spacing of vert grid points in data array
Engine Type		From Jane's or ICAO, retrieved by George Noel according to tail number
Near pwr %		% power setting of engine closest to the lidar
Far pwr %		% power setting of engine farthest from the lidar
ST	m^2 / (Mm sr)	Integrated (i.e., total) enhanced backscatter in the 2-D gridded data from the sweep
ymean	m	horiz dist of the spatial mean of the horiz profile (signal-weighted mean location)
shor	m	sq root of the signal-weighted spatial variance in the horiz about xmean
ε1ssh		Normalized absolute diff between horiz profile points and Gaus. equation with parameters ST, xmean, and shor
ε2ssh		Sq root of normalized squared diff between horiz profile points and Gaus. equation with parameters ST, xmean, and shor
γ1hor		skewness of horiz backscatter profile - the usefulness of these parameters has not yet been evaluated
γ2hor		kurtosis of the horiz bacskcatter profile - the usefulness of these parameters has not yet been evaluated
zmean	m	vert dist above the runway of the spatial mean of the 2-D gridded data (signal-weighted mean location)
sver	m	sq root of the signal-weighted spatial variance in the vert about the zmean
ε1ssv		Normalized absolute diff between vert profile points and Gaus. fit using preceding three parameters
ε2ssv		Sq root of normalized squared diff between vert profile points and Gaus. fit using preceding three parameters
γ1ver		skewness of vert backscatter profile - the usefulness of these parameters has not yet been evaluated
γ2ver		kurtosis of the vert bacskcatter profile - the usefulness of these parameters has not yet been evaluated
ymedian	m	horiz dist from the lidar to the location of the signal-weighted median of the horiz profile
smedh	m	horiz std dev of distribution assuming Gaus. shape possessing dhor
ε1mdh		Normalized absolute diff between horiz profile points and Gaus. equation with parameters ST, xmed, and smedh
ε2mdh		Sq root of normalized squared diff between horiz profile points and Gaus. equation with parameters ST, xmed, and smedh
dhor	m	Signal-weighted absolute deviation in the horiz about xmedian
zmedian	m	vert height above the runway of the location of the signal-weighted median of the vert profile
smedv	m	vert std dev of distribution assuming Gaus. shape possessing dver
ε1mdv		Normalized absolute diff between vert profile points and Gaus. equation with parameters ST, zmed, and smedv
ε2mdv		sq root of normalized squared diff between vert profile points and Gaus. equation with parameters ST, zmed, and smedv
dver	m	Signal-weighted absolute deviation in the vert about zmedian
s68h	m	horiz dist from xmed (avg for the 2 directions) to which the integrated signal is 34.1% of ST, corr. to the std dev of Gaus. distribution
rfn34		Ratio of dist from xmed to where the integrated signal is 34.1% of ST (side farther from lidar div. by corresponding dist on side closer to lidar)
ε168h		Normalized absolute diff between horiz profile points and Gaus. equation with parameters ST, xmed, and s68h
ε268h		sq root of normalized squared diff between horiz profile points and Gaus. equation with parameters ST, xmed, and s68h
s68v	m	vert dist from zmed (avg for the 2 directions) to which the integrated signal is 34.1% of ST, corresponding to the std dev of Gaus. distribution

rtb34		Ratio of the dist from zmed to where the integrated signal is 34.1% of ST on the top divided by the corresponding dist on the bottom
ε168v		Normalized absolute diff between vert profile points and Gaus. equation with parameters ST, vmed, and s68v
ε268v		sq root of normalized squared diff between vert profile points and Gaus. equation with parameters ST, zmed, and s68v
STpth	m^2 / (Mm sr)	Total backscatter (area under the curve) of Gaus. equation with parameters Shmax, xpeak, and spth
ypeak	m	horiz dist from the lidar of STpth
spth	m	std dev of a dist assuming Gaus. shape and based on dist from xpeak (avgd for the 2 directions) where horiz signal profile first is < Shmax/10
rfnpth		Ratio of dist from ypeak to where the integrated signal drops to 1/10 on side farther from lidar divided by corresponding dist on side closer to lidar
ε1pth		Normalized absolute diff between horiz profile points and Gaus. equation with parameters STpth, xpeak, and spth
ε2pth		sq root of normalized squared diff between horiz profile points and Gaus. equation with parameters STph, xpeak, and spth
Shmax	m / (Mm sr)	Peak backscatter in the horiz profile of enhanced backscatter
STptv	m^2 / (Mm sr)	Total backscatter (area under the curve) of Gaus. equation with parameters Svmax, zpeak, and sptv
rtbpth		Ratio of the dist from zpeak to where the integrated signal drops to 1/10 on the top divided by the corresponding dist on the bottom
zpeak	m	Height above the runway of the peak in the vert profile, i.e. location of Svmax
sptv	m	std dev of distribution assuming Gaus. shape and based on dist from zpeak (avgd for the 2 directions) where vert signal profile first is < Svmax/10
ε1ptv		Normalized absolute diff between vert profile points and Gaus. equation with parameters STptv, zpeak, and sptv
ε2ptv		sq root of normalized squared diff between vert profile points and Gaus. equation with parameters STpv, zpeak, and sptv
Svmax	m / (Mm sr)	Peak backscatter in the vert profile of enhanced backscatter
STGh(ext)	m^2 / (Mm sr)	Total backscatter (area under the curve) of Gaus. equation least-squares fitted to the horiz profile, extended with zero values on both ends
yGh(ext)	m	dist from lidar to the spatial mean location of Gaus. equation least-squares fitted to the horiz profile, extended with zero values on both ends
sGh(ext)	m	Spatial std dev of the Gaus. equation least-squares fitted to the horiz profile, extended with zero values on both ends
ε1Gh(ext)		Normalized absolute diff between horiz profile points and Gaus. equation with parameters STGh, xGh, and sGh
ε2Gh(ext)		sq root of normalized squared diff between horiz profile points and Gaus. equation with parameters STGh, xGh, and sGh
STGv(ext)	m^2 / (Mm sr)	Total backscatter (area under the curve) of Gaus. equation least-squares fitted to the vert, extended with zero values on both ends
zGv(ext)	m	dist above the runway of spatial mean location of Gaus. equation least-squares fitted tovert profile, extended with zero values on both ends
sGv(ext)	m	Spatial std dev of the Gaus. equation least-squares fitted to the vert profile, extended with zero values on both ends
ε1Gv(ext)		Normalized absolute diff between vert profile points and Gaus. equation with parameters STGv, xGv, and sGv
ε2Gv(ext)		sq root of normalized squared diff between vert profile points and Gaus. equation with parameters STGv, xGv, and sGv
STGv	m^2 / (Mm sr)	Same as for STGv(ext), but with the actual vert profile (no extension)
zGv	m	Same as for zG(ext), but with the actual vert profile (no extension)
sGv	m	Same as for sGv(ext), but with the actual vert profile (no extension)
ε1Gv		Same as for ε1Gv(ext), but with the actual vert profile (no extension)
ε2Gv		Same as for ε2Gv(ext), but with the actual vert profile (no extension)
STDGh	m^2 / (Mm sr)	Total bkscatter (area under curve) of double Gaus. eqn with equal amp each mode least-sqs fitted to horiz profile, ext with zero values, both ends
yDGh1	m	dist from the lidar to the center of the closer Gaus. in the double-Gaus. fit
yDGh2	m	dist from the lidar to the center of the farther Gaus. in the double-Gaus. fit
sDGh	m	std dev of both Gaus.s in the double-Gaus. fit
ε1DGh		Normalized absolute diff between horiz profile points and the double Gaus. fit
ε2DGh		sq root of normalized squared diff between horiz profile points and the double Gaus. fit
STFGv	m^2 / (Mm sr)	Total bckscatter (area under curve above runway) of a folded Gaus. equation fitted to vert profile, extended with zeroes on upper end
zFGv	m	Height parameter above the runway of the folded Gaus. fit
σFGv	m	std dev parameter of the folded Gaus. fit
ε1FGv		Normalized absolute diff between the folded Gaus. fit and the points in the vert profile
ε2FGv		sq root of normalized squared diff between the folded Gaus. fit and the points in the vert profile
se	1/(mM)	Ambient extinction coefficient used to process the lidar data
<βh>	1/(mM sr)	Haze (aerosol) backscatter coefficient in the foreplume region calculated from lidar signal, calibration, extinction correction, and subtracting sm
sh	1/(mM)	Ambient haze (aerosol) extinction coefficient = se - sm
βm	1/(mM sr)	Molecular backscatter coefficient for air density calculated from surface temperature and pressure
sm	1/(mM)	Molecular extinction coefficient for air density calculated from surface temperature and pressure
Tp	m	vert integral of plume optical depth assuming diff in ambient signal from postplume and foreplume regions is due only to plume attenuation
Lp	Mm sr / m	Plume's lidar extinction-to-backscatter ratio based on Tp and ST

Nabove		Number of beams in the sweep above the plume as designated by the operator in sweep processing
Δτabove		Optical depth between foreplume and postplume regions for the Tp beams if their avg diff in ambient signal were caused by extinction
Δ sh above	1/(mM)	avg extinction coefficient corresponding to Δtabove
r1	m	dist between lidar and near boundary of foreplume region
r2	m	dist between lidar and boundary dividing the foreplume and plume regions
r3	m	dist between lidar and boundary dividing the plume and postplume regions
r4	m	dist between lidar and far boundary of postplume region
F2D	m^2/(Mm sr)^2	Parameter for calculation soot emission based on statistics of plume density - usefulness not evaluated yet
FqR	m^2/(Mm sr)^2	Parameter for calculation soot emission based on statistics of plume density - usefulness not evaluated yet
STqR	m^2/(Mm sr)	Parameter for calculation soot emission based on statistics of plume density - usefulness not evaluated yet
Fq1		Parameter for calculation soot emission based on statistics of plume density - usefulness not evaluated yet
STq1		Parameter for calculation soot emission based on statistics of plume density - usefulness not evaluated yet
# Tp grids		Number of Δz levels occupied by the Tp beams